ADVANCED HEALTHCARE MATERIALS

Supporting Information

for *Adv. Healthcare Mater.*, DOI 10.1002/adhm.202400675

A Biodegradable Fiber Calcium Ion Sensor by Covalently Bonding Ionophores on Bioinert Nanoparticles

Sihui Yu, Chengqiang Tang, Sijia Yu, Wenjun Li, Jiajia Wang, Ziwei Liu, Xinheng Yan, Liyuan Wang, Yiqing Yang, Jianyou Feng, Jiaqi Wu, Kailin Zhang, Hang Guan, Yue Liu, Songlin Zhang, Xuemei Sun and Huisheng Peng*

Supporting Information

for

A Biodegradable Fiber Calcium Ion Sensor by Covalently Bonding Ionophores on Bioinert Nanoparticles

Sihui Yu, Chengqiang Tang, Sijia Yu, Wenjun Li, Jiajia Wang, Ziwei Liu, Xinheng Yan, Liyuan Wang, Yiqing Yang, Jianyou Feng, Jiaqi Wu, Kailin Zhang, Hang Guan, Yue Liu, Songlin Zhang, Xuemei Sun, Huisheng Peng*

Table of Contents

Supplementary Figures

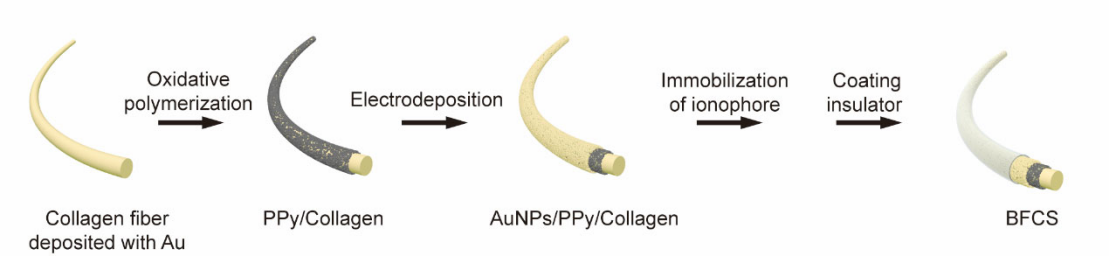

Figure S1. The fabrication process of the BFCS.

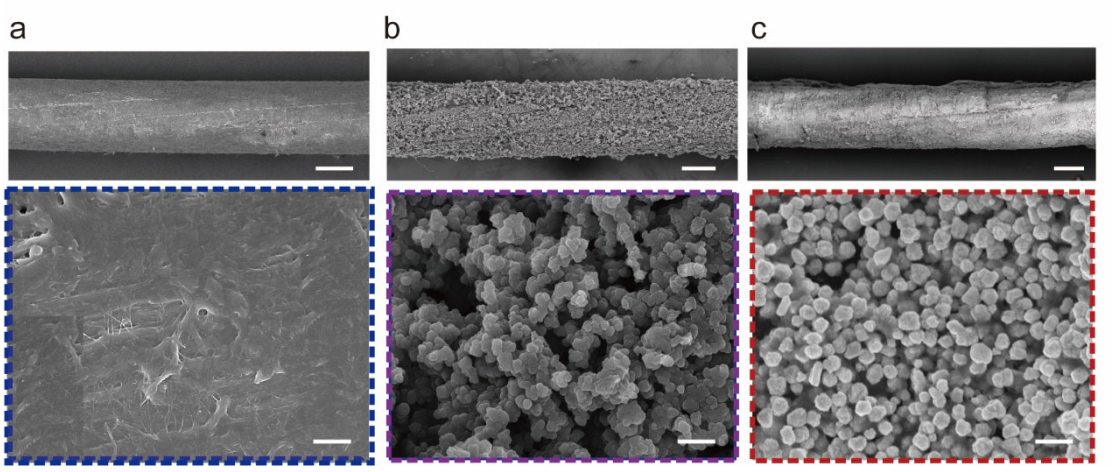

Figure S2. Scanning electron microscopy (SEM) images at low (top) and high (bottom) magnification of collagen fiber deposited with gold (a), PPy/collagen (b), and AuNPs/PPy/collagen (c). Scale bars, 50 μm (top) and 300 nm (bottom).

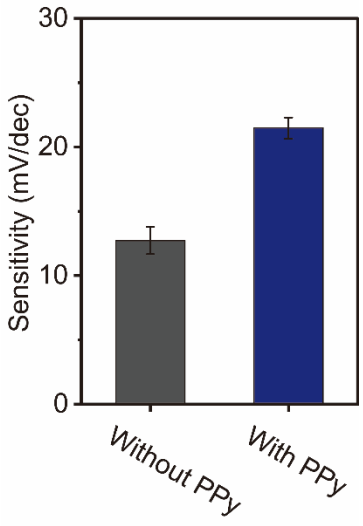

Figure S3. The sensitivity of BFCS with and without PPy.

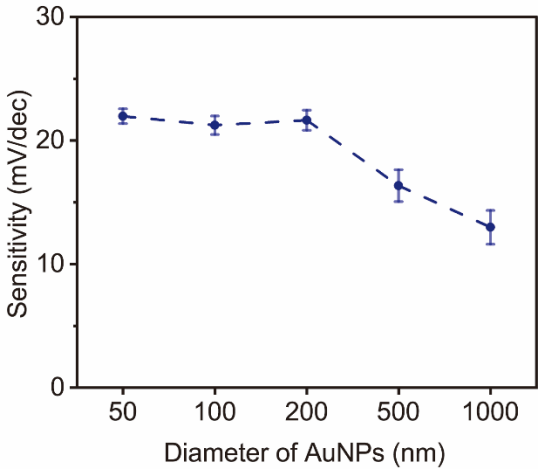

Figure S4. The sensitivity of the BFCS changes with the diameter of AuNPs.

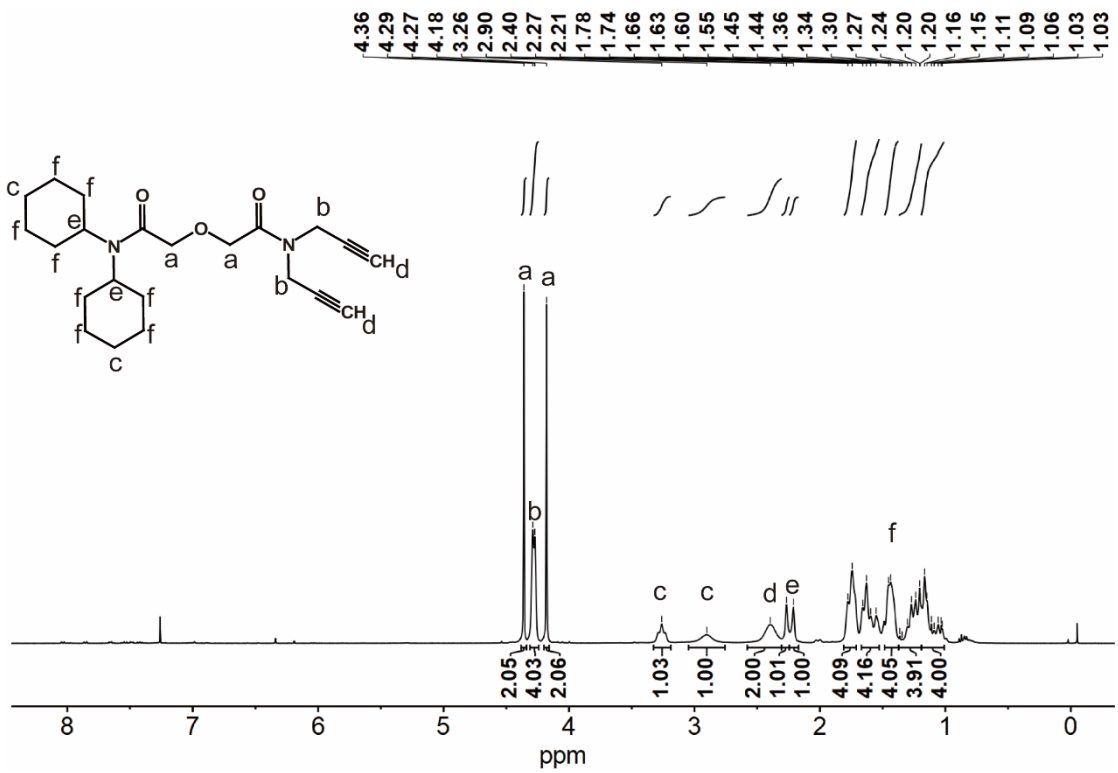

Figure S5. ^{1}H NMR of the Ca^{2+} ionophore. ^{1}H NMR (400MHz, $CDCl_3$, ppm): δ 4.36 (s, 2H), 4.28 (d, *J* = 6.5 Hz, 2H), 4.18 (s, 2H), 3.26 (t, *J* = 11.3 Hz, 1H), 2.90 (s, 1H), 2.40 (s, 2H), 2.27 (s, 1H), 2.21 (s, 1H), 1.76 (d, *J* = 13.3 Hz, 4H), 1.78–1.03 (m, 18H).

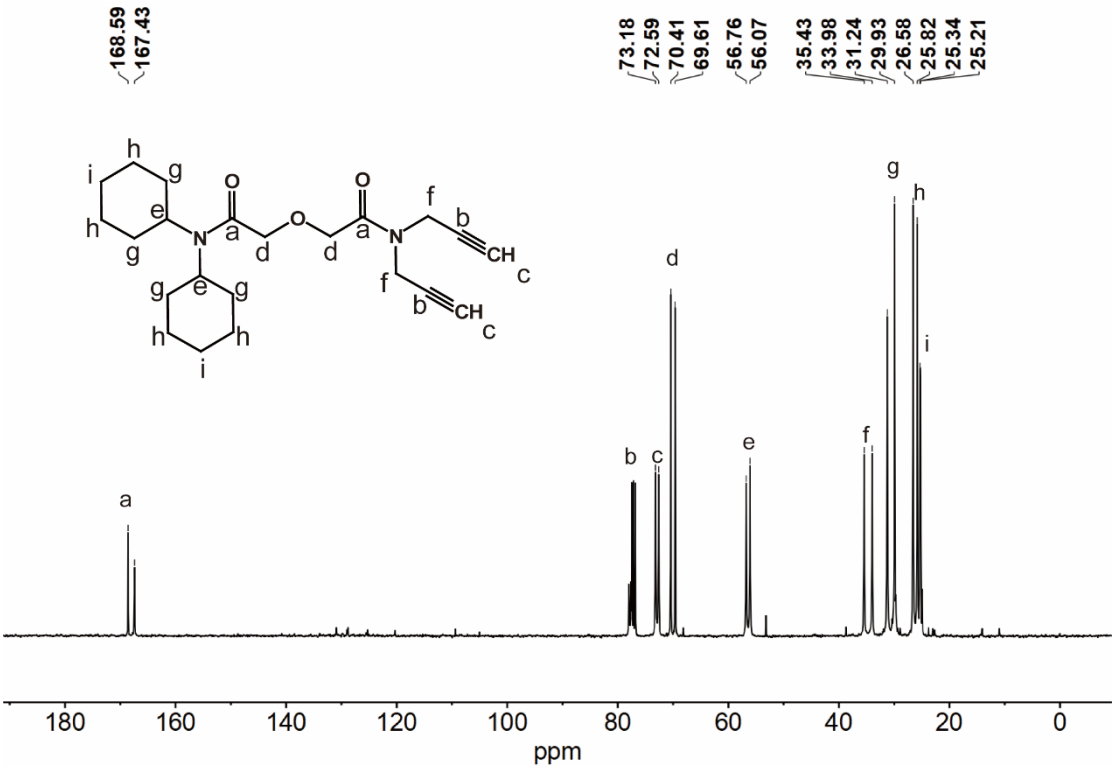

Figure S6. ^{13}C NMR of the Ca^{2+} ionophore. ^{13}C NMR (400MHz, $CDCl_3$, ppm): δ 168.59, 167.43, 77.79, 77.64, 73.18, 72.59, 70.41, 69.61, 56.76, 56.07, 35.43, 33.98, 31.24, 29.93, 26.58, 25.82, 25.34, 25.21.

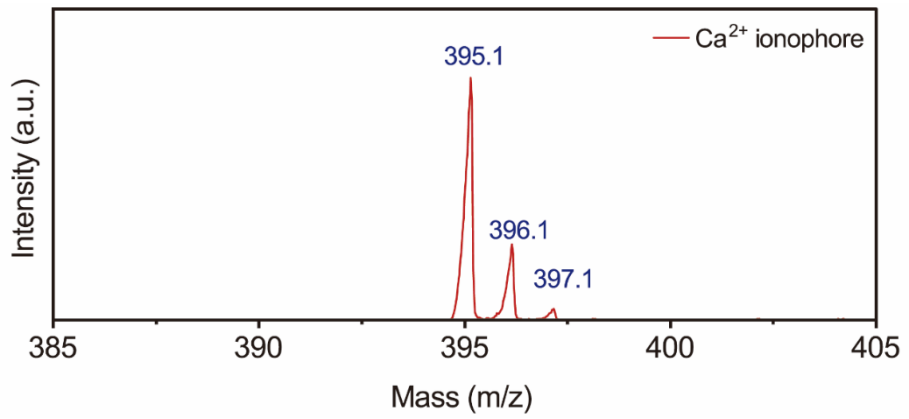

Figure S7. Mass spectrum (MS) of the Ca^{2+} ionophore. MS for $C_{22}H_{32}N_2NaO_3$ was found to be 395.1.

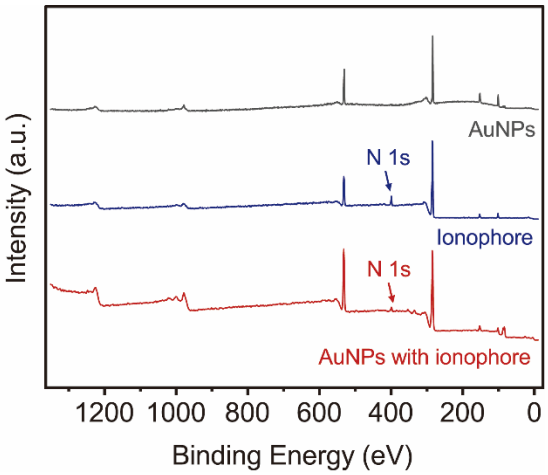

Figure S8. Full X-ray photoelectron spectrometer spectra of AuNPs, Ca^{2+} ionophore, and AuNPs with ionophore.

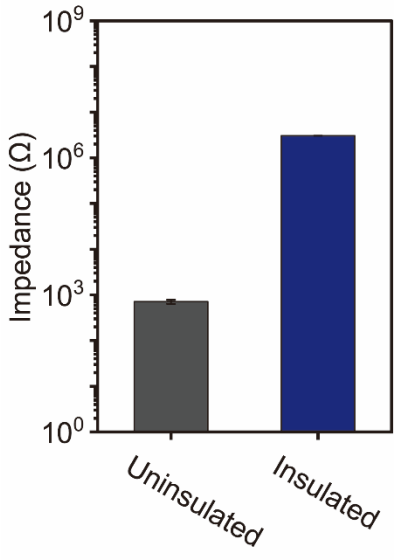

Figure S9. The impedance of the electrodes at 1000 Hz before and after insulation.

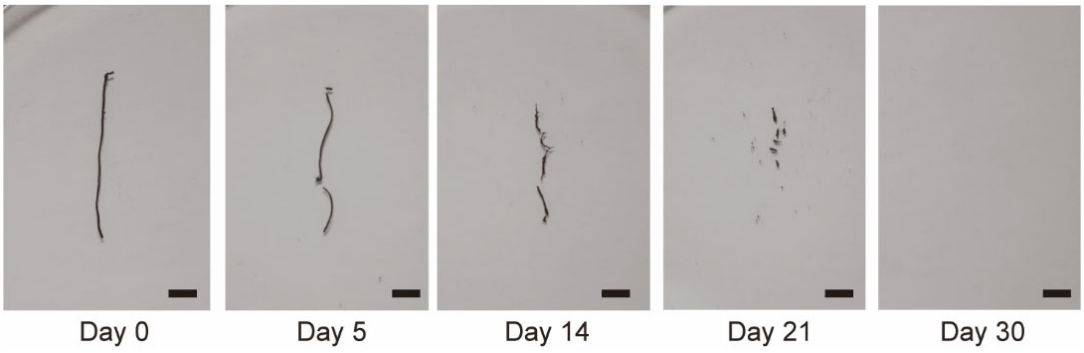

Figure S10. Photographs of the BFCS during degradation process in PBS. Scale bars, 3 mm.

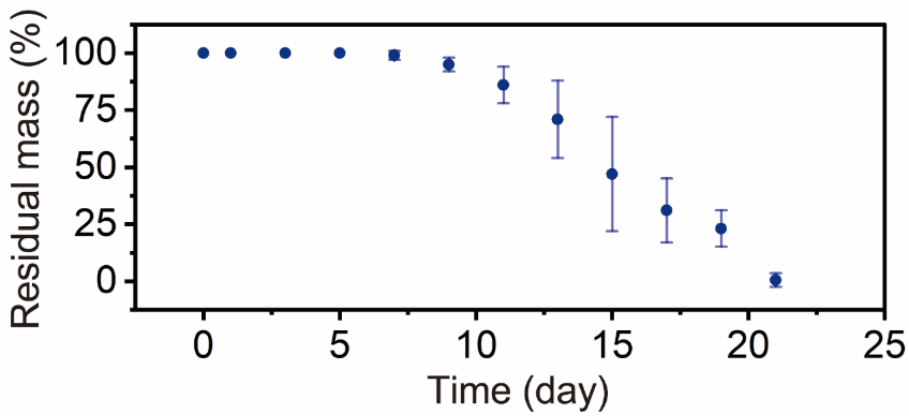

Figure S11. The weight changes of the BFCS soaked in normal saline with time. Error bars show the mean ± SD (n = 3).

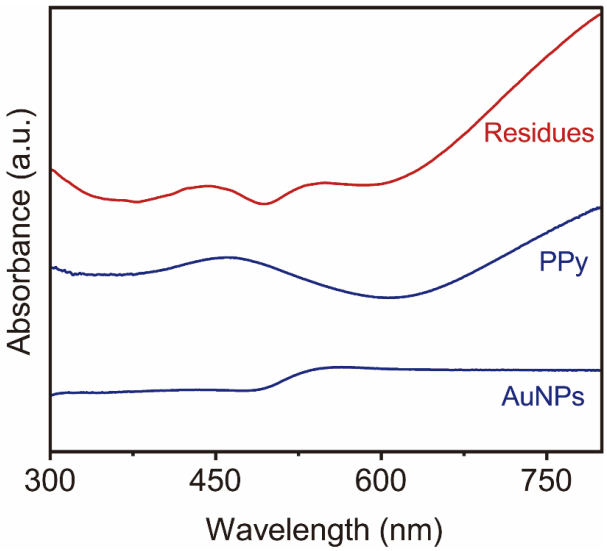

Figure S12. Ultraviolet-visible (UV-Vis) spectra of the residues, bare PPy and bare AuNPs, indicating the residues were composed of PPy and AuNPs.

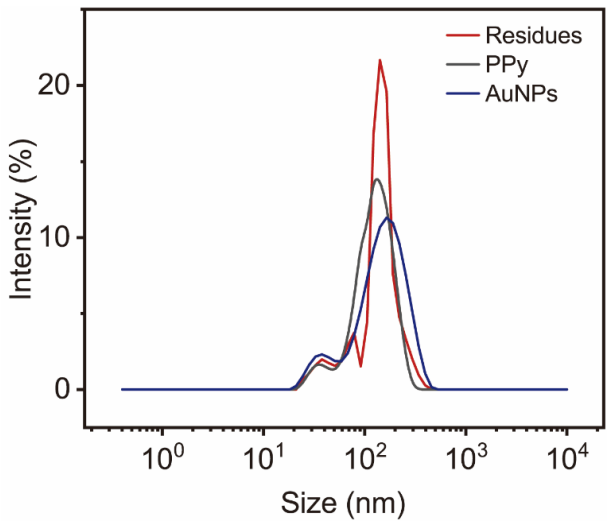

Figure S13. Dynamic light scattering (DLS) spectra of the residues, bare PPy and bare AuNPs. The grain size was 100–300 nm.

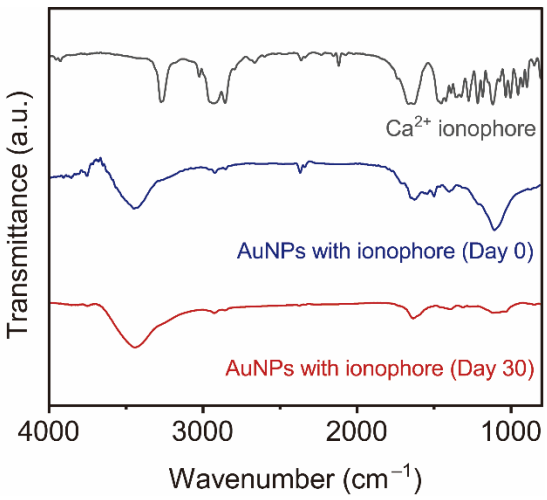

Figure S14. Infrared spectra of Ca^{2+} ionophore and AuNPs with ionophore before and after the degradation of BFCS.

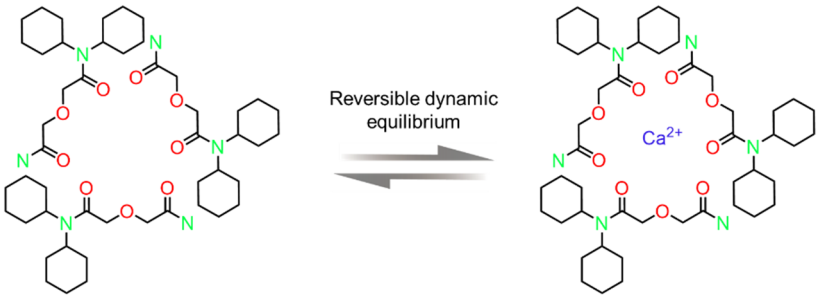

Figure S15. The molecular schematic diagram of the reversible dynamic equilibrium absorption between ionophores and Ca^{2+}.

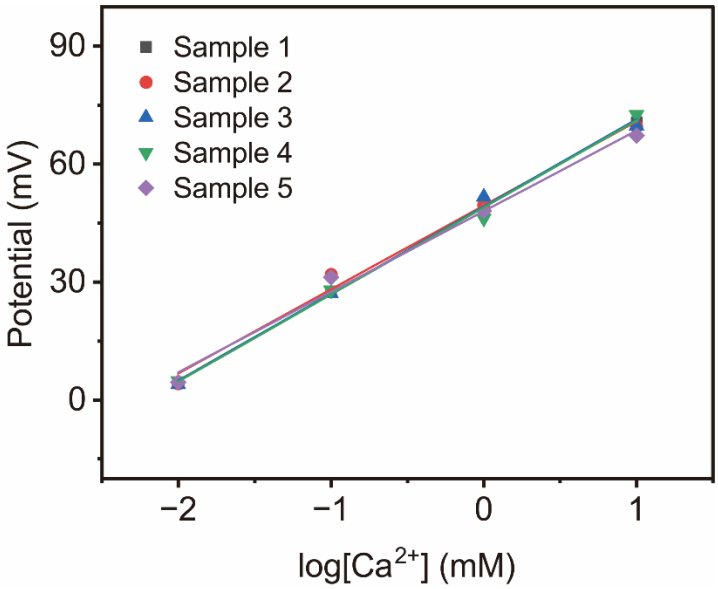

Figure S16. The reproducibility of BFCS in the same batch.

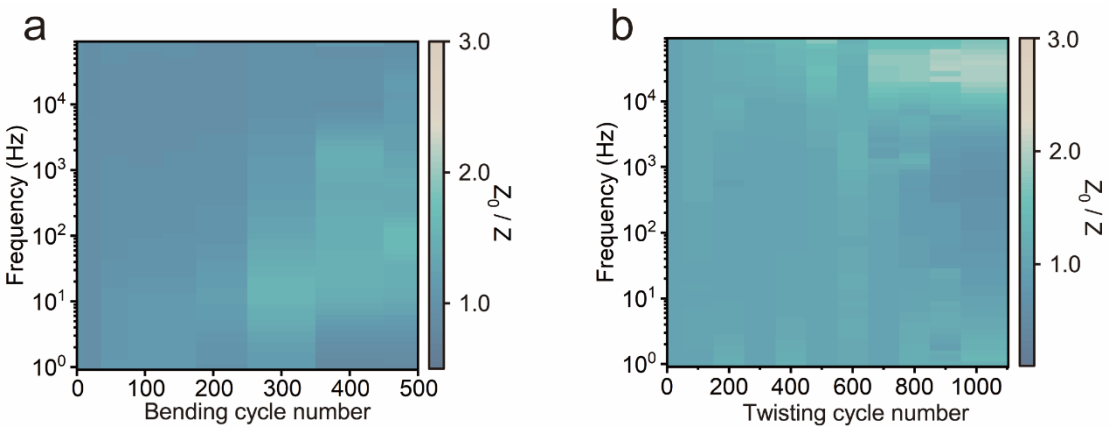

Figure S17. The evolutions of impedance magnitude of BFCS during (a) 500 cycles of bending and (b) 1000 cycles of twisting.

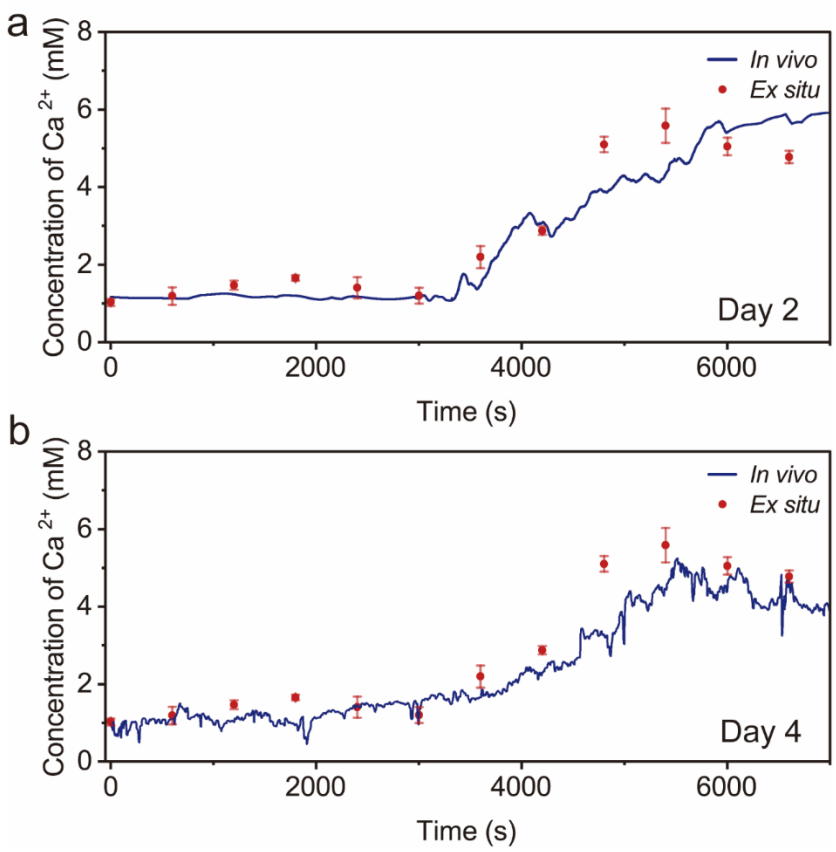

Figure S18. Comparison of *in vivo* and *ex situ* Ca^{2+} concentration results on the 2nd and 4th day after implantation. *In vivo* results were obtained from BFCS continuously and *ex situ* results were measured every 10 minutes. The fitness of *in vivo* and *ex situ* results proved the reliability of BFCS. Error bars showed the mean ± SD of *ex situ* calcium content assay kits results (n = 3).

Figure S19. Digital photographs of the degradation process of BFCS in the subcutaneous region. BFCS gradually disappeared in about 4 weeks. Scale bars, 5 mm.

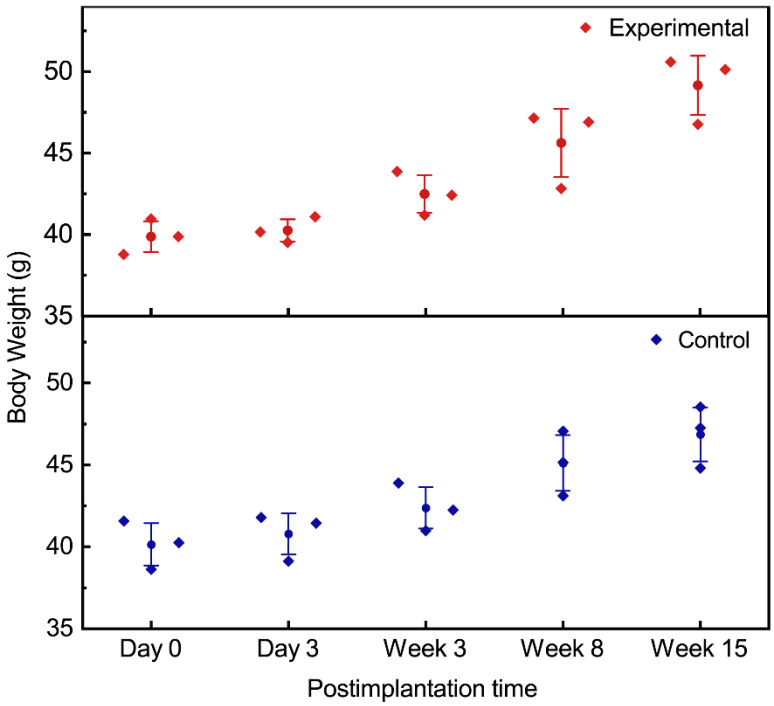

Figure S20. Changes in body weight of experimental (BFCS implanted) and control groups, measured from day 0 to week 15 after implantation. Body weight gradually increased with age in both groups, indicating a healthy condition. Biologically independent animals, n = 3, mean ± SD.

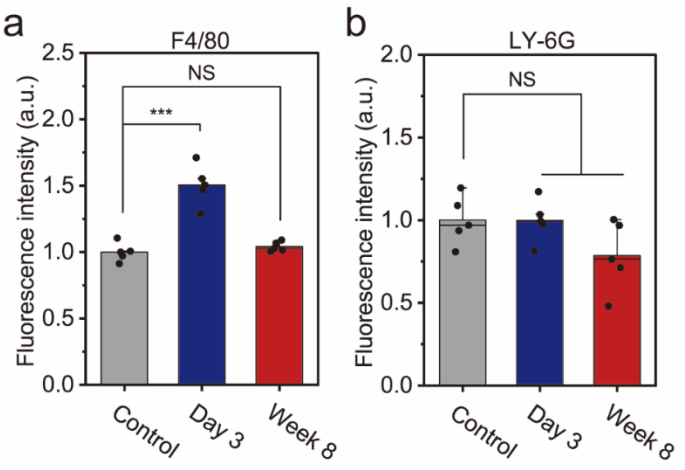

Figure S21. Fluorescence statistics of F4/80 (a) and LY-6G (b) in Figure 4a, showing no significant difference at Week 8. ***$P < 0.001$.

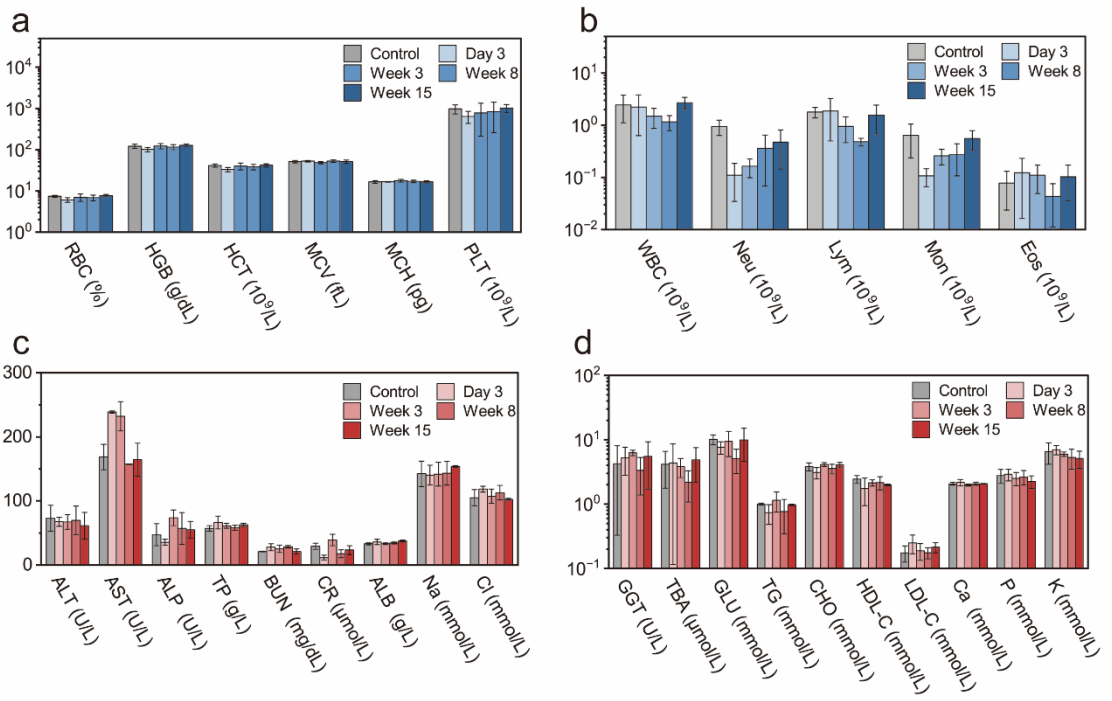

Figure S22. Analysis of complete blood counts and blood chemistry, revealing overall health condition, especially blood physiology. RBC, number of red cells; HGB, hemoglobin; HCT, hematocrit; MCV, mean corpuscular volume; MCH, mean erythrocyte hemoglobin content; PLT, platelet count; WBC, white blood cell; Neu neutrophils; Lym, lymphocyte; Mon, monocytes; Eos, eosinophils; ALT, alanine aminotransferase; AST, aspartate transaminase, ALP, alkaline phosphatase; TP, total protein; BUN, blood urea nitrogen; CR, creatinine; ALB, albumin; Na, sodium; Cl, chlorine; GGT, γ-glutamyl transferase; TBA, total bile acid; GLU, glucose; TG, triglyceride; CHO, cholesterol; HDL-C, high-density lipoprotein cholesterol; LDL-C, low-density lipoprotein cholesterol; Ca, calcium; P, phosphorus; K, potassium. Biologically independent animals, n = 3, mean ± SD.

Supplementary Tables

Table S1. Alternative substrates and insulating materials for BFCS.

Materials of substrate fiber	Lifespan (days)	Degradation time (days)	Data sources
Collagen	**4**	**30**	**This work**
Polyglycolide - lactide (PGLA)	6	50	This work
Polyglycolide acid (PGA)	7	60	This work
Polylactic acid (PLA)	/	>100	*Sci. Adv.* **2021**, 7, eabe3097.
Poly p-dioxanone (PPDO)	/	>100	*J. Polym. Environ.* **2013**, 21, 1088.

Table S2. Comparison of mating rate between BFCS and other ion sensors.

Sensing target	Matching rate	Reference
Ca^{2+}	**~90%**	**This work**
Ca^{2+}	~90%	*Nat. Biomed. Eng.* **2020**, 4, 159.
Ca^{2+}	96.5%	*Angew. Chem. Int. Ed.* **2020**, 59, 10426.
Ca^{2+}	89.5%	*Anal. Chim. Acta.* **2016**, 943, 50.
Fe^{2+}	91.6%	*Angew. Chem. Int. Ed.* **2020**, 59, 20499.
Li^{+}	92.0%	*Lab Chip* **2014**, 14, 1308.